cept at very short times where the bounds and series are practically indistinguishable.

Since the bounds and the truncated Taylor series are based on exactly the same information, it may appear surprising that they disagree over most of the time range. The error must lie in the Taylor series result, since the bounds are rigorous. In truncating the Taylor series, one sets the higher (unknown) terms to zero. This implies that all the higher moments of $I(\omega)$ *vanish,* which is clearly inconsistent with $I(\omega)$ having strictly positive lower even moments. This inconsistency of the truncation procedure results in the truncated Taylor series values lying outside our bounds.

We conclude that our bounding technique for time correlation functions represents a major advance, in both accuracy and reliability, over the Taylor series representation based on the same initial time derivatives. Since we have also proven that our bounds are the best possible on the basis of this information, any further increases in accuracy must make use of some new information or other constraints on the correlation function.

We are grateful to Professor J. C. Wheeler for sending us his moment values prior to publication. One of the authors (O.P.) would like to thank Statens Naturvidenskabelige Forskningsraad, Denmark, for financial support.

*Work supported by the National Science Foundation.

†Permanent address: Chemistry Department, University of Aarhus, Aarhus, Denmark.

[1]R. Kubo, in *Lectures in Theoretical Physics,* edited by W. E. Brittin and L. G. Dunham (Interscience, New York, 1959), Vol. 1, p. 181; R. Zwanzig, Annu. Rev. Phys. Chem. 16, 67 (1965).

[2]L. van Hove, Phys. Rev. 95, 249 (1954).

[3]R. G. Gordon, Advan. Magn. Resonance 3, 1 (1968).

[4]S. Karlin and W. J. Studden, *Tchebycheff Systems: With Applications in Analysis and Statistics* (Wiley Interscience, New York, 1966).

[5]Ref. 4, p. 105.

[6]Ref. 4, p. 101.

[7]R. G. Gordon, J. Math. Phys. (N. Y.) 9, 655 (1968).

[8]G. G. Dantzig, *Linear Programming and Extensions* (Princeton Univ. Press, Princeton, N. J., 1963).

[9]C. Isenberg, J. Phys. C: Proc. Phys. Soc., London 4, 164 (1971), and references therein; J. C. Wheeler and C. Blumstein, to be published.

Breaking and Turbulent Transition in Ion Acoustic Waves

C. N. Judice
Bell Laboratories, Whippany, New Jersey 07981

and

J. F. Decker and R. A. Stern
Bell Laboratories, Murray Hill, New Jersey 07974

(Received 13 November 1972)

New wave-particle processes determining the evolution of large-amplitude, low-frequency ion waves have been observed in numerical and laboratory experiments.

Previous studies of finite-amplitude ion waves have been concerned with hydrodynamic processes, which lead to steepening and soliton formation,[1] or else with wave-particle interactions,[2] notably "trapping." We describe here a new class of wave-particle processes which occur on *time scales intermediate* between those of hydrodynamic and "trapping" processes. These processes can become dominant, leading to final states which are turbulent.[3] Besides their fundamental interest, the processes may have technical importance in recently proposed schemes[4] for wave heating of plasmas.

It is well known[1] that finite-amplitude, low-frequency waves will distort and form a soliton pulse in the breakdown time $t_{br}=1/\omega\epsilon$, where ω is the angular frequency of the launched wave and $\epsilon=\delta n/n$ is the initial ion density perturbation. Wave-particle interactions, however, become important as the number of resonant ions increases; these are the ions which satisfy the inequality $|v-c|\leq(2e\varphi/m_i)^{1/2}$, where v is the ion velocity and φ is the wave potential. This number increases with $(\varphi)^{1/2}$, and also as $T_e/T_i\to 1$, since then the wave phase velocity, $c\cong v_{th}(T_e/T_i+3)^{1/2}$, approaches the ion thermal velocity, $(T_i/m_i)^{1/2}=v_{th}$.

The resonant ions are usually assumed[2] to end up in "trapped" orbits oscillating at the bounce frequency $\omega_B = \omega\epsilon^{1/2}$. We note, first, that at least half the bounce period, $t_{tr} \approx \pi/\omega\epsilon^{1/2}$, must elapse between the instant a wave is launched and the time when "trapping" is established. We next point out that $t_{tr} > t_{br}$ for $\epsilon \gtrsim 0.1$. In this regime, where hydrodynamic distortion can occur prior to trapping, we find that at low T_e/T_i and large $\Delta\varphi$, waves evolve through two distinct phases: (1) a laminar phase characterized by steepening and soliton formation (here called a Korteweg–de Vries process,[1] or KdV), together with ion reflection (RI process) characterized by formation of ion beams within the wave potential troughs, followed by (2) a turbulent transition (TT) phase characterized by instability of the ion beam, and transition of the wave-particle system into intense turbulence.

First, we discuss computer simulations which illustrate ion trajectories during these processes. A hybrid particle-in-cell code[5] was used which treats ions as finite-size particles, and electrons as an isothermal fluid [i.e., $n_e \sim \exp(e\varphi/T_e)$]. In Fig. 1(a) a typical set of ion phase-space plots are given in the wave frame for $\omega = 0.058\omega_{pi}$, $k\lambda_{De} = 0.049$, and $\epsilon = 0.3$, $T_e/T_i = 10$. At $\tau = \omega_{pi}t = 0$ the Maxwellian ion distribution, truncated at $4v_{th}$, is given a density, velocity, and temperature perturbation to launch a single sinusoidal wave with wave number k. This gives the spatially averaged distribution $\bar{F}$ in Fig. 1(b) a distorted shape.

By a breakdown time $\tau = 46.9$ the KdV process is nearly complete, as evidenced by the severe distortion of the waveform, while the RI process begins to become important as the wave breaks in phase space. At $\tau = 108$ the mean distribution shows the formation of a dense, narrow beam moving at $v_B/c = 1.56$. As the beam rides up the potential ramp of the wave, its velocity is reduced enough to interact with the plasma via a local ion-beam–plasma instability before trapping diffuses the beam. This is clear in Fig. 1(a) at $\tau = 250$ when the beam-plasma system decays into a turbulent state as the characteristic phase-space vortices of beaming instabilities are formed. At the tail of the beam we see the slower ions "turned around" before local instability sets in. Therefore, in this experiment the start of trapping and instability occur simultaneously.

In Fig. 2 we plot for the same numerical experiment the field energy, $E = (8\pi T_i)^{-1}\int k^2\varphi^2 dx$, versus time for selected spectral components of the

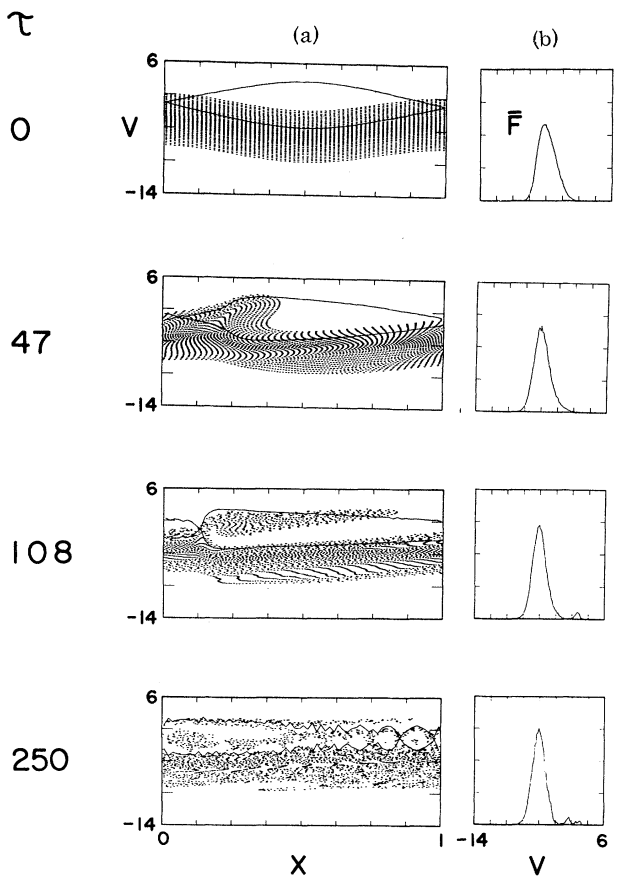

FIG. 1. Ion phase-space plots. (a) Particle position and velocity plotted with the self-consistent phase space separatrix between resonant and nonresonant ions. Initially 5% of the ions are resonant. (b) Mean ion distribution averaged over the 64 cells. V is the velocity (v/v_{th}), X the space coordinate $(128\times\lambda_{De})$, and $\bar{F}$ the mean ion distribution.

distorted wave. Wave-wave coupling during the KdV process causes a rapid growth of the harmonics at the expense of the fundamental. The growth of the lower harmonics is slowed by the ion reflection process, since a pure KdV state would have the energy in wave $2k$ grow an order of magnitude larger relative to the fundamental.[6] The short-wavelength harmonic at $9k$ saturates at $\tau = 80$ and then begins to grow again during the TT phase. This additional growth can be attributed to the instability: If we solve the linear dispersion relation[7] for the beam-plasma system, where a 10% beam is moving at $v_B/c = 1.23$ (at $\tau \approx 200$), one obtains a growth rate $\gamma_{9k} = 0.036\omega_{pi}^{-1}$ which agrees well with the experiment.

Parallel experiments were performed in the laboratory with a double plasma device 30 cm in

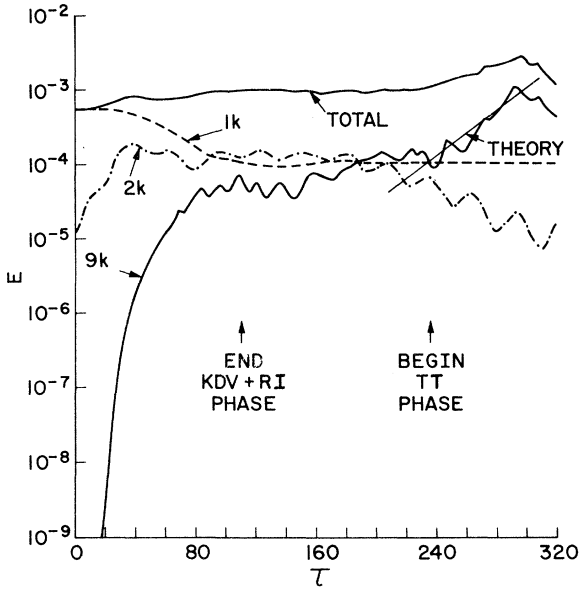

FIG. 2. Potential-energy curves. Logarithmic plot of field energy E versus time, for the duration of the run, for the fundamental, second, and a higher harmonic corresponding to the fastest-growing beam-plasma instability mode.

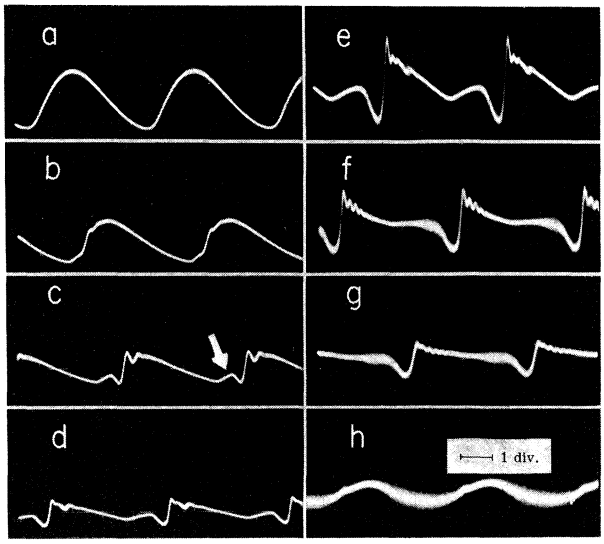

FIG. 3 Potential profiles of breaking waves. Horizontal: time, 10 μsec/div. Vertical: Langmuir probe output, (a)–(d) 0.2 V/div., (e)–(h) 0.05 V/div.; probe dc output corresponding to $n = 1.0$ V. Probe position relative to launching plane: (a) 4.86 cm, (b) 6.72 cm, (c) 8.58 cm, (d) 10.44 cm, (e) 12.30 cm, (f) 16.02 cm, (g) 19.74 cm, and (h) 15.95 cm (increased excitation).

diameter and length, operated at $n_e \sim 2\times10^9$ cm^{-3} ($\omega_{pi}/2\pi \sim 1.4$ MHz), $T_e \sim 1.6$ eV and $T_i \sim 0.3$ eV, with neutral pressures $\sim 2\times10^{-4}$ Torr of argon. Collision lengths were of the order of the machine dimensions. Excitation and dc bias conditions were chosen to avoid the production of accelerated free-streaming ions, as verified through energy analysis of the ions.

The evolution of a wave at 25 kHz ($\omega = 0.015\omega_{pi}$) with $\epsilon = 0.2$ is shown in Fig. 3. Close to the launching plane the wave potential is sinusoidal with a slightly steepened leading edge, as in Fig. 3(a). The leading soliton in Fig. 3(b) emerges about 20 μsec ($\sim 0.6t_{br}$) after launch, as expected. The beginning of the RI process is evident from the emergence of a bump in front of the soliton, seen in Fig. 3(c). Sampled energy analysis reveals this to be a distinct beam, as in the numerical experiment, moving at $\sim 1.5c$ and spreading as shown in Figs. 3(d) and 3(e).

Following the KdV and RI processes, it is seen in Figs. 3(f) and 3(g) that the density in the beam region acquires a random, high-frequency behavior, without affecting the structure of the laminar wave front. The instability is localized in the beam. In the case $\epsilon = 0.2$, a laminar wave front is eventually re-established, although at much reduced amplitude. However, at larger excitation, e.g., $\epsilon = 0.3$, the laminar wave eventually loses its substructure, and a hybrid structure consisting of a laminar carrier and supposed turbulence propagates, as shown in Fig. 3(h).

Figure 4 shows the spectra resulting from these processes. At low excitation levels only a harmonic line spectrum appears, as in Fig. 4(a). With increasing excitation, a broad underlying continuum develops. Eventually the spectrum separates into a low-frequency regime dominated by a harmonic line structure, and an intense high-frequency continuum peaked near $0.4\omega_{pi}$ with a half-width of about $0.2\omega_{pi}$, as shown in Fig. 4(c). The absence of low-frequency turbulence is consistent with the fact that, here, the energy cascade originates with segmented beams whose length is much shorter than the fundamental wavelength. This contrasts with ion sound turbulence driven by continuous beams,[3] which has no line components, but appreciable low-frequency continuum. As a measure of turbulent intensity, we find $(\delta n/n)^2 \sim 6\times10^{-4}$ for $\epsilon \approx 0.4$; this compares well with intensities $(1-3)\times10^{-3}$ achieved[3] with beams whose density amounts to 10% of the plasma.

The spatial evolution of the turbulent component at 500 kHz is shown in Figs. 4(d)–4(f). It grows steeply, peaks at 15 cm and maintains a

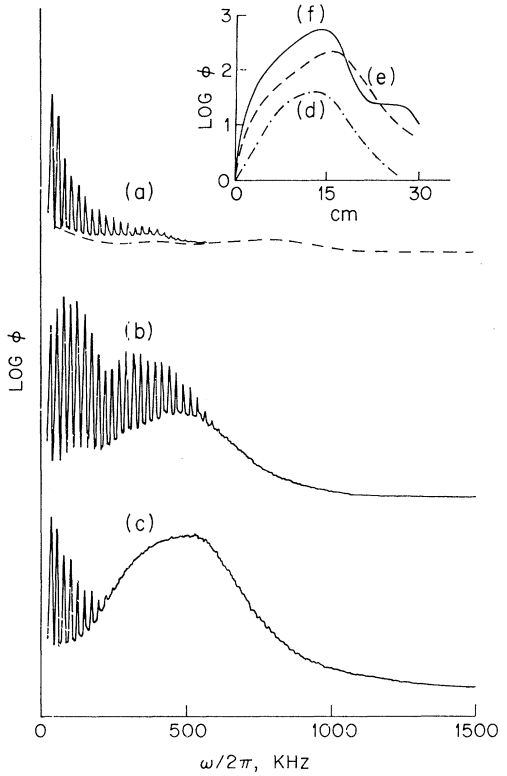

FIG. 4. Turbulent spectra of hybrid waves (a)–(c) at 18 cm from grid (presented with vertical offset). Initial excitations: (a) $\epsilon = 0.06$ (0.15 V), (b) $\epsilon = 0.14$ (0.35 V), and (c) $\epsilon = 0.28$ (0.7 V). (d)–(f) Evolution of 500-kHz component. (d) $\epsilon = 0.14$ (0.35 V), (e) $\epsilon = 0.2$ (0.5 V), and (f) $\epsilon = 0.4$ (1.0 V). Vertical scales in arbitrary units.

large intensity throughout the plasma. In contrast, beam-excited turbulence peaks near the point of entrance (e.g., 4 cm under similar conditions[3]), because the driving beam thermalizes rapidly. This suggests that, by adjusting the breaking length $L_{br} = c/\omega\epsilon$, the wave-generated turbulence can penetrate the plasma in a controlled manner, optimizing energy transfer from waves to particles.[4] This is confirmed by sampling the ion energy distribution in the turbulent region. Over a broad range of energies near the fundamental-wave phase velocity, the number of "hot" ions was observed to increase appreciably.

In a recent experiment[8] on the stability of shock fronts against externally imposed modifications of the plasma ahead of the front, it was noted that sinusoidal wave trains in unmodified plasmas could also become unstable. We can now check whether the processes described here could have been operative. We find that the relevant parameters for the wave trains were $\omega/\omega_{pi} \approx O(10^{-2})$, $T_e/T_i < 10$, and $\epsilon = 0.18$, which are in the right regime.

In summary, we have pointed out the physical parameters of a regime in which hydrodynamic and wave-particle interactions occur on differing time scales, and presented theoretically and experimentally examples demonstrating that new processes can intervene and dominate the stability of ion waves.

We gratefully acknowledge discussions with N. Marcuvitz, R. J. Mason, B. Rosen, G. Schmidt, and F. Tappert.

[1]V. E. Zakharov, Zh. Prikl. Mekh. Tekh. Fiz. 3, 167 (1964); N. J. Zabusky and M. D. Kruskal, Phys. Rev. Lett. 15, 240 (1965); H. Washimi and T. Taniuti, *ibid.* 17, 996 (1966); D. Montgomery, *ibid.* 19, 1465 (1967); S. G. Alikhanov, R. Z. Sagdeev, and P. Z. Chebotaev, Zh. Eksp. Teor. Fiz. 57, 1565 (1969) [Sov. Phys. JETP 30, 847 (1970)]; F. D. Tappert and C. N. Judice, Phys. Rev. Lett. 29, 1308 (1972).

[2]E.g., nonlinear Landau damping in H. Ikezi and Y. Kiwamoto, Phys. Rev. Lett. 27, 718 (1971); S. Takamura and T. Okuda, Phys. Lett. 39A, 91 (1972); and trapping in Y. Kawai and H. Ikegami, Plasma Phys. 13, 463 (1971); W. M. Manheimer and R. W. Flynn, Phys. Fluids 14, 2393 (1971); H. Ikezi, Y. Kiwamoto, K. Nishikawa, and K. Mima, *ibid.* 15, 1605 (1972); N. I. Budka, V. I. Karpman, and D. R. Shklyar, Zh. Eksp. Teor. Fiz. 61, 1463 (1971) [Sov. Phys. JETP 63, 778 (1972)]; J. M. Dawson, B. Rosen, and W. L. Kruer, Plasma Physics Laboratory, Princeton University Report No. Matt-883, 1972 (unpublished).

[3]The final states are quite different from "trapping" instabilities, instead they are similar to ion acoustic turbulence recently reported in D. R. Baker, Phys. Rev. Lett. 28, 1189 (1972); R. J. Taylor and F. V. Coroniti, *ibid.* 29, 34 (1972).

[4]R. P. H. Chang, M. Porkolab, and B. Grek, Phys. Rev. Lett. 28, 206 (1972); W. L. Kruer, J. Katz, J. Byers, and J. DeGroot, Phys. Fluids 15, 1613 (1972).

[5]R. J. Mason, Phys. Fluids 14, 1943 (1971); C. N. Judice, Bull. Amer. Phys. Soc. 16, 1279 (1971).

[6]C. N. Judice, Ph. D. dissertation, Stevens Institute of Technology, 1972 (unpublished).

[7]S. Abas and S. P. Gary, Plasma Phys. 13, 262 (1971).

[8]R. A. Stern and J. F. Decker, Phys. Rev. Lett. 27, 1266 (1971).

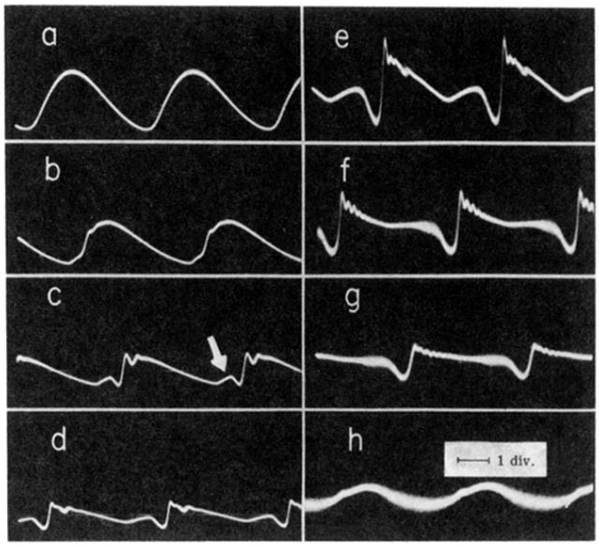

FIG. 3 Potential profiles of breaking waves. Horizontal: time, 10 μsec/div. Vertical: Langmuir probe output, (a)–(d) 0.2 V/div., (e)–(h) 0.05 V/div.; probe dc output corresponding to $n = 1.0$ V. Probe position relative to launching plane: (a) 4.86 cm, (b) 6.72 cm, (c) 8.58 cm, (d) 10.44 cm, (e) 12.30 cm, (f) 16.02 cm, (g) 19.74 cm, and (h) 15.95 cm (increased excitation).